Asian Journal of Scientific Research

ISSN 1992-1454

science alert
http://www.scialert.net

ANSInet
an open access publisher
http://ansinet.com

Asian Journal of Scientific Research 7 (1): 18-32, 2014
ISSN 1992-1454 / DOI: 10.3923/ajsr.2014.18.32

An Efficient ANFIS based Approach for Screening of Chronic Obstructive Pulmonary Disease (COPD) from Chest CT Scans with Adaptive Median Filtering

[1]K. Meenakshi Sundaram and [2]C.S. Ravichandran
[1]Department of Information Technology, Dhanalakshmi Srinivasan College of Engineering, Coimbatore, India
[2]Department of Electrical and Electronics Engineering, Sri Ramakrishna Engineering College, Coimbatore, India

Corresponding Author: K. Meenakshi Sundaram, Department of Information Technology, Dhanalakshmi Srinivasan College of Engineering, Coimbatore, India

ABSTRACT

Medical diagnostic and imaging system are ubiquitous in modern health care facilities. The advantages of early detection of potential lesions and suspicious masses within the bodily tissue have been well established. It can be detected and assessed many different types of injuries, diseases and conditions with the aid of the medical imaging that allows medical personnel to look into living cells non-instructively. Chronic Obstructive Pulmonary Disease (COPD) is the fourth leading cause of death worldwide and the only chronic disease with increasing mortality rates. COPD is the name for a group of lung diseases including chronic bronchitis, emphysema and chronic obstructive airways disease. This study involves in improving the accuracy over the existing technique using the adaptive region growing property and Adaptive-Neuro-Fuzzy Inference System-ANFIS classifier. Initially, pre-processing is carried out for the input image by Adaptive median Filter technique to make the image suitable for further processing. The contours of the image will be obtained using region growing technique. The ANFIS classifier is then used to confirm the suspected COPD cavities. The classification will be carried out by the features which have been taken from the segmented image. The proposed technique is implemented in MATLAB and the performance is compared with the existing technique. From the experimental result it can be said that the proposed method achieved more accuracy as compared with existing techniques.

Key words: Chronic obstructive pulmonary disease (COPD), medical imaging, ANFIS classifier, adaptive median filter, local gabor XOR pattern

INTRODUCTION

The Medical imaging is one of the most useful diagnostic tools available in modem medicine. Medical diagnostic and imaging system are ubiquitous in modern health care facilities. The advantages of early detection of potential lesions and suspicious masses within the bodily tissue have been well established. COPD is a most important disease but under-recognized cause of morbidity and mortality worldwide (Pauwels and Rabe, 2004). The occurrence of COPD in the general population is predictable to be, ~1% across all ages rising steeply to >10% amongst those aged 40 years. The occurrence climbs appreciably higher with age. The 30-yr for the global increase in COPD is from 1990-2020 is surprising. COPD is projected to move from the sixth to the third most common cause of death worldwide, at the same time as rising from fourth to third in terms of

morbidity within the same time-frame (Murray and Lopez, 1997). The cofactors in charge for this extraordinary increase are the continued use of tobacco, coupled with the changing demographics of the world, such that many more people, especially those in developing countries, are living into the COPD range of age.

COPD occurrence is generally higher than recognized by health authorities (Pauwels *et al*., 2001; http://www.goldcopd.org/). Few population-based occurrence surveys have been carried out and prevalence estimates have repeatedly relied on expert opinion or self-reported doctor diagnosis, a disreputably unpredictable source of information for COPD. For example, in the USA National Health and Nutrition Examination Survey III, 70% of those with airflow obstruction had never received the diagnosis of COPD (Stang *et al*., 2000). The IBERPOC study in Spain also reported that there was no previous diagnosis of COPD in 78% of identified cases and, even more worrisome, only 49% of those with severe COPD were receiving some kind of treatment for COPD (Pena *et al*., 2000). Recently, the Nippon COPD Epidemiology (NICE) study in Japan, presented the current series, had a similar finding (Fukuchi *et al*., 2004).

During the 1990s, surveys of asthma successfully identified a huge variations in asthma occurrence in children and adults, as high as 20-fold. It shows that the geographical distribution of COPD is more harmonized than asthma, at least in the developed countries. It seems that the distribution of COPD follows the distribution of its risk factors very closely, of which smoking is undoubtedly the most important worldwide. COPD is in the spotlight of worldwide at the high prevalence, morbidity and mortality present challenges for healthcare systems. From the patient's viewpoint, it is also a disease that has a reflective effect on quality of life (Rennard *et al*., 2002). The burden of COPD can be assessed in a number of ways such as mortality, morbidity, prevalence, disability-adjusted life years, cost and quality of life. A number of authors have reviewed this topic in detail elsewhere (Viegi *et al*., 2001; Loveymi *et al*., 2011; Malik *et al*., 2008).

In this study, first the input image is pre-processed; the lung region is segmented from that image, segmented the cavity region in that lung region, extracted some features for training the classifier and used the ANFIS classifier to identify the tuberculosis affected lung. The pre-processing is done by using the Adaptive Median Filter to avoid the noise in the input image and to increase the image quality. The cavity segmentation is done by evaluating the pixel range in the segmented lung region and setting a threshold value from that evaluated pixels and comparing every pixel with that threshold value. After the lung and cavity segmentation, some parameters are chosen to train the classifier to identify whether an x-ray image is a normal or tuberculosis affected. The classifier used in proposed technique is ANFIS classifier. The ANFIS Classifier is then trained using the parameters chosen from the sample chest CT scan images to identify the normal lung and tuberculosis affected lung.

RELATED WORK

The Computer-aided Diagnosis (CAD) system is used for early detection of tuberculosis in lungs by analyzing chest 3D Computed Tomography (CT) images. The underlying idea of developing a CAD system is not to delegate the diagnosis to a mechanism, but quite than a machine algorithm acts as a support to the radiologist and points out locations of suspicious objects, so that the overall sensitivity is raised. CAD systems meet four main objectives which are improving the quality and accuracy of diagnosis, increasing therapy success by early detection of cancer, avoiding unnecessary biopsies and reducing radiologist interpretation time (Magesh *et al*., 2011).

Katoch (2004) explained that the diagnosis of tuberculosis is mostly based on clinical features, demonstration of Acid Fast Bacilli (AFB) and isolation of Mycobacterium tuberculosis from the clinical specimens. These techniques have limits of speed, warmth and specificity. Several rapid techniques for detection of early growth have been described for last two decades which can help in obtaining the culture and sensitivity reports early. Important among such methods are BACTEC, Mycobacterial Growth Indicator Tuber (MGIT) and Septi-chek, MB/BacT systems. This growth can be recognized by rapid methods based on lipid analysis and specific gene probes, PCR-RFLP methods and ribosomal RNA sequencing. Advance improvement in knowledge about genetic structure of tubercle bacillus helps to develop gene probes and gene amplification methods for detection of tubercle bacillus, from culture or directly in clinical specimens and molecular detection of drug resistance. The gene probes can help in rapid identification of isolates, gene amplification methods developed for diagnosis of tuberculosis are obviously highly sensitive especially in culture negative specimens from different paucibacillary forms of disease. The molecular methods drug resistant mutants for drugs like rifampicin can be detected with reasonable certainty within hours. In recent years great advances have been made in Computer Aided Diagnosis (CAD) systems for detecting disease from Computed Tomography scans, mainly due to the advances made in the scanning machines which allow a greater amount and quality of information to be extracted during a single breath of the patient. The use of textural analysis and pattern recognition techniques for regression or classification is most suited to the evaluation of global conditions (e.g., Ground glass, Emphysema) rather than local (small nodules) which won't be concerned with in this report. This recent progress in CAD in Chest Radiology has been discussed in Giger *et al.* (2001), where it has been noted that the amount of 3-D image data from thoracic CT scans greatly increases the number of images that much be reviewed by the radiologist and therefore a search aid may be a great benefit.

Uchiyama *et al.* (2003) said that the selected regions in 315 HRCT images from 105 patients, relating to six different patterns, i.e., ground-glass opacities, reticular and linear opacities, nodular opacities, honeycombing, emphysematous change and consolidation, labeled by 3 radiologists. The lungs were first segmented, using standard technique, then divided into many contiguous regions of interest (ROIs) with a 32×32 matrix and classified using artificial neural networks. The accuracy varied from 88 to 100%, with specificity in detecting a normal ROI of 88.1%.

Sluimer *et al.* (2003) and Loveymi *et al.* (2011) presented a CAD system to automatically distinguish normal from abnormal tissue in HRCT chest scans of 116 patients, producing 657 ROIs labeled as containing normal or abnormal tissue. The circular ROIs with an 80-pixel diameter were extracted from the peripheral lung region in slices at the height of the aortic arch, with each ROI required to contain at least 75% abnormal tissue. An accuracy of 86.2% as obtained, comparable to those of a radiologist when evaluating only the ROIs, i.e., without seeing the whole scan.

Lee *et al.* (1997) explained that the digital CT is a technique used for recording images in computer code as an alternative of on X-ray film. The images are displayed on a computer monitor can be enhanced or lightened or darkened before they are printed on film. Images can also be manipulated; the radiologist can magnify or zoom in on an area. This screening will generate large number of CT images to be determined by a small number of radiologists resulting in misdiagnosis due to human errors caused by visual fatigue. The sensitivity of human eye decreases with increasing number of images. Hence, it may be helpful for a radiologist, if a computer-aided system is used for detection of tumours in CT images. Computer-aided detection (CAD) involves the use of

computers to bring suspicious areas on a CT to the radiologist's attention. It is used after the radiologist has done the initial review of the CT. There are several image processing methods proposed for extract of tumours from CT image for better view of area and shape of tumour.

PROPOSED TECHNIQUE FOR THE IDENTIFICATION OF CAVITY

The block diagram of the proposed approach is shown in Fig. 1. In this figure some sample chest CT scan images are taken with COPD and without COPD. The sample images are then preprocessed and then send for segmentation process. There segmenting the lung and cavity regions. After the lung and cavity regions are segmented from the sample images, some parameters are chosen to train the classifier. First the preprocessing is done to find weather the COPD is affected or not. After the preprocessing process, need to segment the lung and the cavity region. After that the chosen parameters are given to the classifier, here the ANFIS classifier is used. The ANFIS classifier then identify whether the input chest CT scan image is affected by COPD or not by comparing the parameters from the sample images and from the input image.

Pre-processing: The input image is subjected to the pre-processing steps to make the image suitable for further process. The pre-process is used to load the input image to the MATLAB environment and it will remove the noise present in the input image. The image is passed through the Adaptive median filter to lower the noise and to get a better image. The adaptive median filter will also increase the image quality and the corner of the images.

Adaptive median filter: The standard median filter performs well as long as the spatial noise density of the salt and pepper noise is not large. The filter performance degrades when the spatial noise variance of the salt and pepper noise increases (Chen and Whu, 1998). Further with larger image and as the size of the kernel increases, the details and the edges becomes obscured (Maragos and Schafer, 1987). The standard median filter does not take into account the variation of image characteristics from one point to another. The behavior of adaptive filter changes based on statistical characteristic of the image inside the filter region defined by the m×n rectangular window S_{xy} (Maragos and Schafer, 1987). The adaptive median filter differs from other adaptive filter as the size of the rectangular window S_{xy} is made to vary depending on:

- Z_{min} = Minimum gray level value in S_{xy}
- Z_{max} = Maximum gray level value in S_{xy}
- Z_{med} = Median of gray level in S_{xy}
- Z_{xy} = Gray levels at coordinate (x,y)
- S_{max} = Maximum allowed size of S_{xy} Gonzalez and Woods (2002)

The flowchart of adaptive median filtering is based on two levels is shown in Fig. 2.

The adaptive median filtering algorithm works in two levels, denoted by level 1 and level 2. The application of AMF provides three major purposes: To denoise images corrupted by salt and pepper (impulse) noise; to provide smoothing of non-impulsive noise and also to reduce distortion caused by excessive thinning or thickening of object boundaries. The values Z_{min} and Z_{max} are considered statistically by the algorithm to be 'impulse like' noise components, even if these are not the lowest and highest possible pixel values in the image.

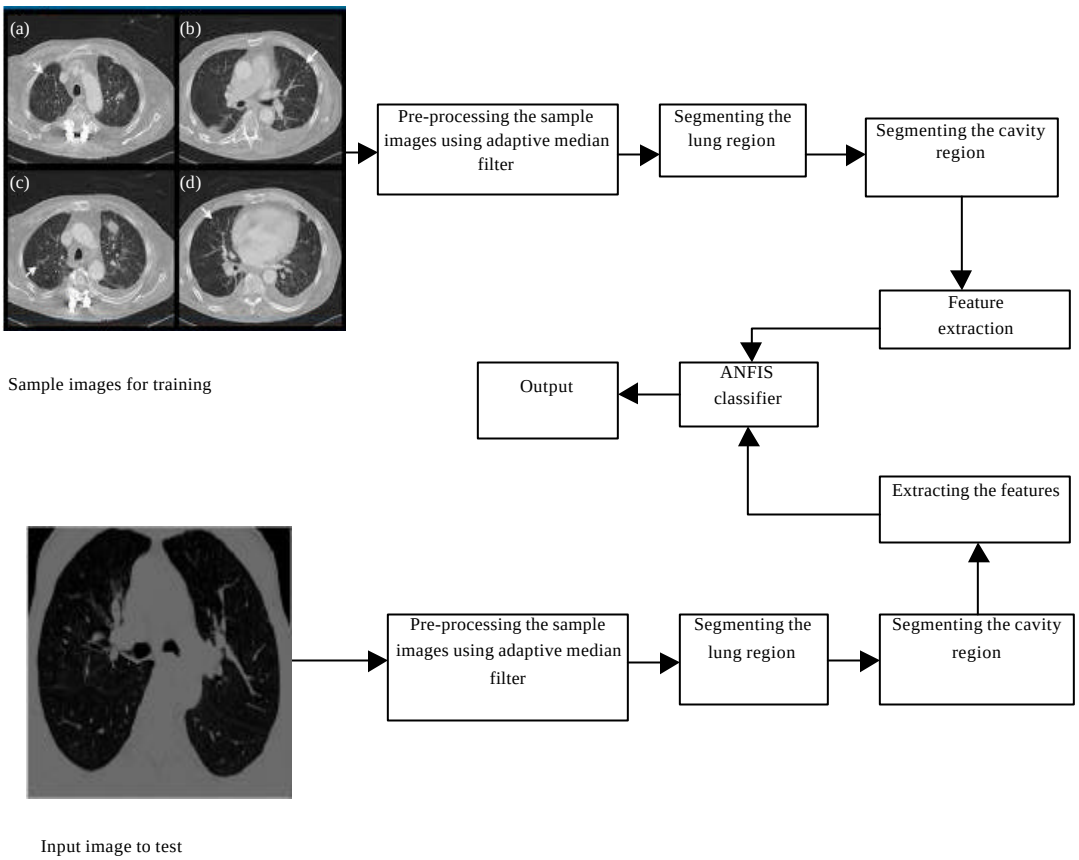

Fig. 1: Block diagram for proposed technique

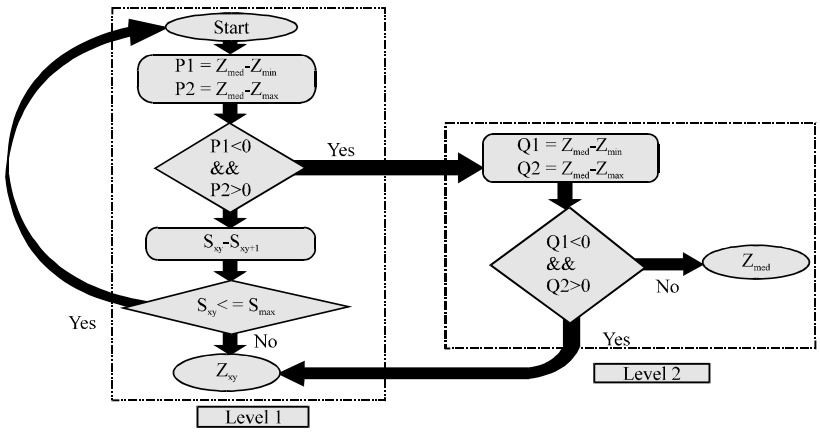

Fig. 2: Flowchart of adaptive median filter

The purpose of LEVEL1 is to determine if the median filter output Z_{med} is impulse output or not. If level 1 does find an impulse output then that would cause it to branch to level 2. Here, the algorithm then increases the size of the window and repeats level 1 and continues until it finds a median value that is not an impulse or the maximum window size is reached, the algorithm returns

0	-1	0
-1	4	-1
0	-1	0

-1	-1	-1
-1	8	-1
-1	-1	-1

Fig. 3: Two commonly used discrete approximations to the adaptive median filter

the value of Z_{xy}. Every time the algorithm outputs a value, the window S_{xy} is moved to the next location in the image. The algorithm is then reinitialized and applied to the pixels in the new location. The median value can be updated iteratively using only the new pixels, thus reducing computational overhead.

Two commonly used small kernels are shown in Fig. 3. Because these kernels are approximating a second derivative measurement on the image, they are very sensitive to noise. To counter this, the image is often smoothed before applying the Adaptive median filter. This pre-processing step reduces the high frequency noise components prior to the differentiation step.

Lung segmentation: Lung segmentation is a process of segmenting the lungs from the chest CT scan image. The normal process of region growing technique for segmenting the lungs is shown in Fig. 4. First choose a pixel from the chest CT scan image as default. Then need to set a threshold value for comparison to find the pixel intensity for the lung area in the chest CT scan. The default pixel which chosen is compared with the adjacent pixel values. If the difference between the default pixel and the adjacent pixel is greater than the threshold value, have to exclude that adjacent pixel. If the difference between the default pixel and the adjacent pixel is less than the threshold value, have to include that adjacent pixel for region growing. Compare all the pixels except the left pixels with its adjacent pixels by keeping one pixel as default. The process of normal region growing technique is shown in the Fig. 4.

In this study, comparing the normal region growing technique with the Local Gabor XOR Pattern (LGXP) based region growing technique to segment the lungs from the chest CT scan image. The LGXP technique is used to find the texture image.

The LGXP based region growing technique is as follows. In LGXP technique, apply the Gabor Phase Technique on every pixel in the chest CT scan image. The Gabor Phase Technique will convert all the pixel values to phase values (0 to 360). After converting all the pixel values to phase values, find these phase values comes under which quadrant. Each quadrant has certain values. For the first quadrant the value is zero and for the second quadrant the value is one and for the third quadrant the value is two and for the fourth quadrant the value is three. After that choose a default phase value of a pixel and check under which quadrant this phase value comes and assign respective quadrant value to that pixel. After assigning respective quadrant value to the default pixel, check the adjacent pixel's phase values and assign the respective quadrant values to those adjacent pixels. Then convert the adjacent pixel's value as zero which has the same quadrant value of the default pixel. If the adjacent pixels value does not have the same quadrant

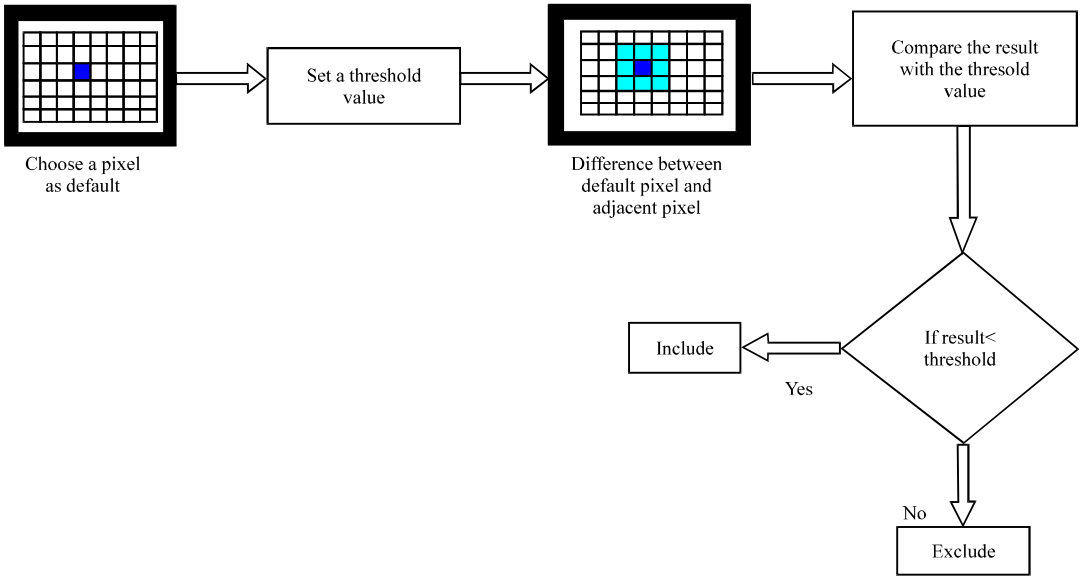

Fig. 4: Block diagram of normal region growing technique

value of the default pixel, convert the adjacent pixel's value as one. Now the pixel values would be like binary values as zeros and ones. After converting the pixel values as binary format, make that binary format as decimal value and apply that decimal value to the default pixel. The process of taking the binary value is shown in the figure. Likewise apply this LGXP process for all the pixels in the chest CT scan by keeping one pixel as default. The sample process of LGXP technique is shown in Fig. 5.

The fundamental idea of technique (Xie *et al*., 2010) is to ease the sensitivity of Gabor phase to the differing positions, whether two phases reflect same local feature must be determined in a "looser" way. Specifically, if two phases belongs to the same interval (for instance: 00, 900), they are believed to have similar local features or else they reflect different local features. In this section, the LGXP descriptor is presented.

Figure 6 shows an instance for the LGXP encoding method where the phase is quantized into 4 ranges. In LGXP technique, phases are first quantized into disparate ranges and the LGXP operator is applied to the quantized pixels of the central pixel and each of its neighboring pixels and eventually the result of the binary labels are concatenated together as a local pattern of the central pixel. In the Fig. 6a is the matrix with initial phase of the pixels after applying the Gabor filter and Fig. 6b is the result after quantization and Fig. 6c is the result after XOR comparison with the center quantized value. From the matrix which we got after XOR comparison, we can deduce the binary value obtained is 01011101 and its equivalent decimal value is 93. The pattern of LGXP in binary and decimal form is as follows:

$$LGXP_{\mu v}(P_c) = \left(LGXP_{\mu v}^{N}, LGXP_{\mu v}^{N-1}, \ldots\ldots\ldots\ldots\ldots LGXP_{\mu v}^{1}\right)\text{binary} = \left[\sum_{i=1}^{N} 2^{i-1}.LGXP_{\mu v}^{i}\right]_{\text{decimal}}$$

where, P_c denotes the central pixel in the Gabor phase map with scale v and orientation , N is the size of the neighborhood and:

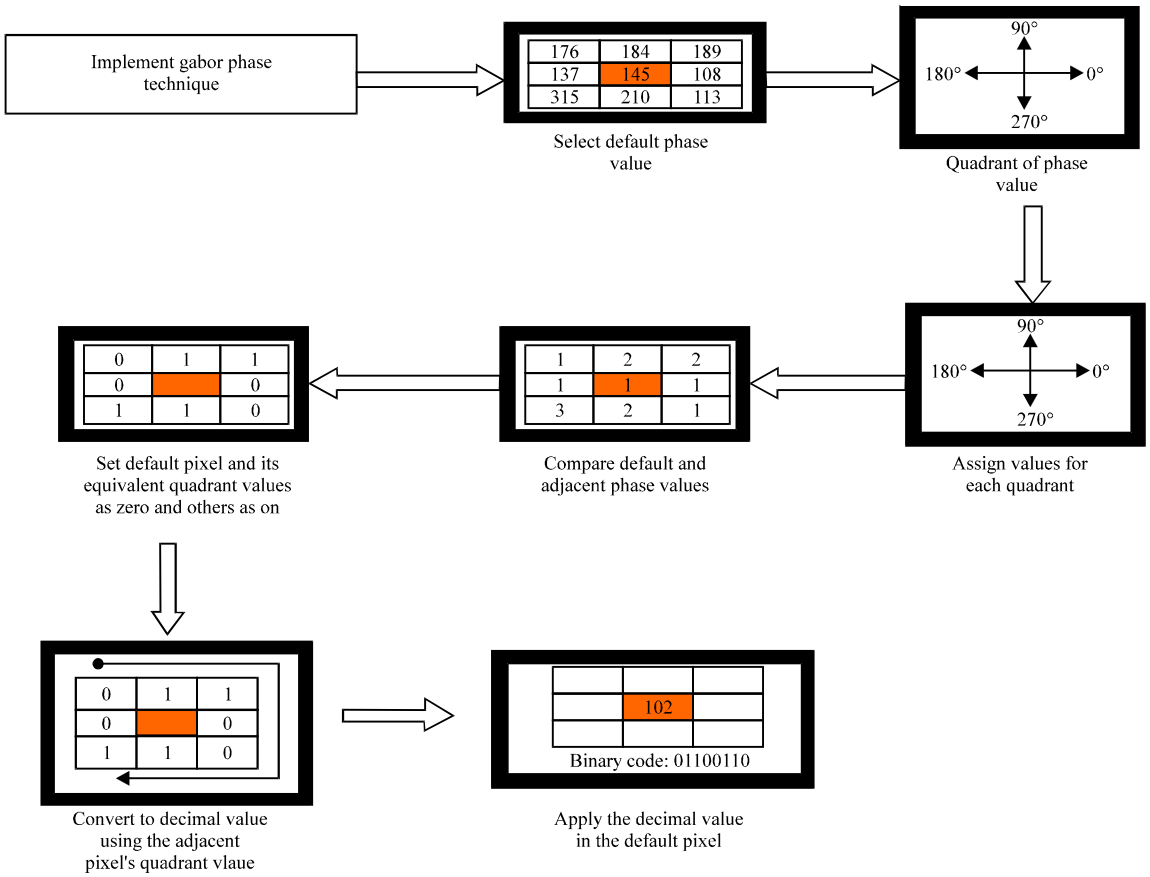

Fig. 5: Block diagram of LGXP Technique Local Gabor XOR Pattern (LGXP)

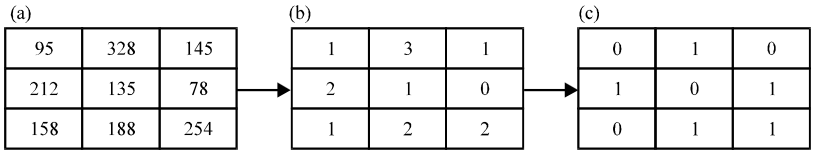

Fig. 6(a-c): Example of LGXP method where the phase is quantized into 4 ranges, (a) Matrix with initial phase of the pixels after applying the Gabor filter, (b) Result after quantization and (c) Rresult after XOR comparison with the center quantized value

$$LGXP_{\mu v}^{1}\left(i=1,2,.....,N\right)$$

denotes the pattern calculated between P_c and its neighbor P_i which is computated as follows:

$$LGXP_{\mu v}^{1}=q\left(\Phi_{\mu v}\left(P_c\right)\right)\otimes q\left(\Phi_{\mu v}\left(P_i\right)\right),i=1,2,.....,N$$

where, $\phi_{\mu v}$uv denotes the phase, denotes the LXP operator which is based on XOR operator, q denotes the quantization operator which calculates the quantized code of the phase according to the number of phase ranges:

$$a \otimes b = \begin{cases} 0, \text{ if } a = b \\ 1, \text{ else} \end{cases}$$

$$q\left(\phi_{\mu v}(.)\right) = i, \text{if } \frac{360 * i}{e} \le \Phi_{\mu v}(.) < \frac{360 * (i+1)}{e}, \quad i = 0,1,.....b-1$$

where, e denotes the number of phase ranges. With the pattern explained above, one pattern map is computed for each Gabor kernel. Thereafter, each pattern map is split into m non overlapping sub blocks and the histograms of all the sub blocks of scales and the orientations are concatenated to form the proposed LGXP descriptor of the input face image:

$$H = \left(H_{\mu Ovo1},.....,H_{\mu Ovom},.....,;H_{\mu O-1vs-1}1;,.....,H_{\mu O-1vs-1m}\right)$$

where, $H_{\mu v}$ (I = 1, 2,... ., m) denotes the histogram of the i^{th} sub block of the LGXP map with scale v and orientation.

Cavity segmentation: After the lung segmentation, identify the cavities in the lung. The cavities present in the lung region are an essential thing to identify the COPD affected lung. To identify the cavity in the lung, set an adaptive threshold value. The threshold value is chosen by calculating the pixel range in the lung region and dividing that pixel range by two. After that, compare the threshold with all the pixels. While comparing the pixels to the threshold value, if the pixel value is greater than the threshold value then it would be the cavity region and if the pixel value is less than the threshold value then it would be the lung region. Figure 7 shows the block diagram for segmenting the cavity region from the lung region.

Feature extraction: After finding the regions, extract some features to diagnose the disease in the lung. To discover the disease in the lung, have to feed the extracted feature into the classifier, because the extracted features will give vital information about the region which is used to train the classifier. In this study an ANFIS classifier is used for feature extraction. The features need to extract are number of cavities in the lung region, minimum area of cavity region, maximum area of cavity region, total number of pixels in each cavity, maximum repeated pixel intensity in the cavity region and maximum repeated pixel in the lung region to find the total number of cavities in the lung region. Because the normal lung would also have some cavities present in its region. So to distinguish the normal lung image and the COPD affected lung should find the total numbers of cavities present in the lung region and give the result to the ANFIS classifier.

Adaptive neuro-fuzzy inference system (ANFIS) classifier

Architecture of ANFIS: The ANFIS is a fuzzy Sugeno model put in the structure of adaptive systems to make easy learning and adaptation (Jang, 1993). Such structure makes the ANFIS modeling more efficient and less reliant on expert knowledge. To present the ANFIS structural design, two fuzzy if-then rules based on a first order Sugeno model are measured:

- **Rule 1:** If (x is A_1) and (y is B_1) then (f1 = $p_1x + q_1y + r_1$)
- **Rule 2:** If (x is A_2) and (y is B_2) then (f2 = $p_2x + q_2y + r_2$)

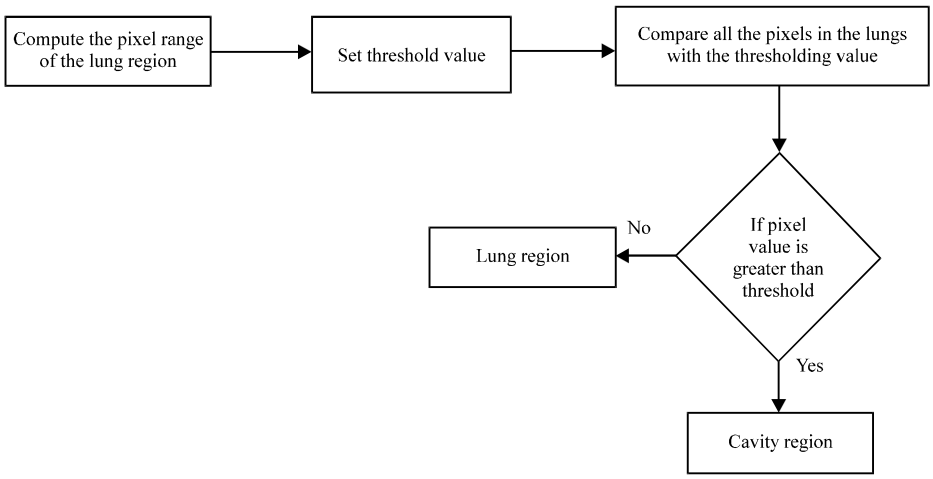

Fig. 7: Block diagram of cavity segmentation

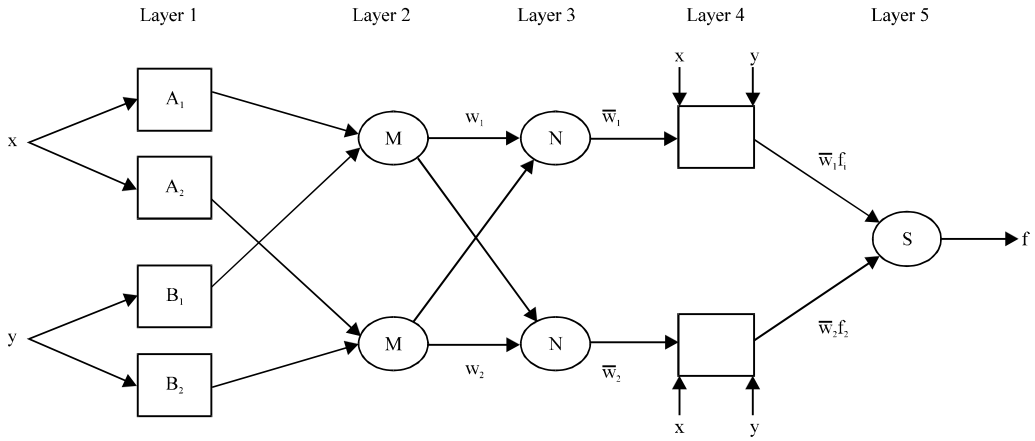

Fig. 8: ANFIS architecture

where, x and y are the inputs, A_i and B_i are the fuzzy sets, f_i are the outputs within the fuzzy region precise by the fuzzy rule, pi; qi and ri are the design parameters that are determined throughout the training process. The ANFIS architecture to put into practice these two rules is shown in Fig. 8, in which a circle indicates a fixed node, while a square indicates an adaptive node.

In the first layer, all the nodes are adaptive nodes. The outputs of layer 1 are the fuzzy membership grade of the inputs which are given by

$$O_i^1 = \mu_{Ai}(x), i=1,2, \tag{1}$$

$$O_i^1 = \mu_{Bi-2}(y), i=3,4 \tag{2}$$

where, $\mu_{Ai}(x)$, $\mu B_{i-2}(y)$ can adopt any fuzzy membership function. For example, if the bell shaped membership function is employed, $\mu_{Ai}(x)$ is given by:

$$\mu_{Ai}(x)=\frac{1}{1+\left\{\left(\frac{x-c_i}{a_i}\right)^2\right\}b_i} \tag{3}$$

where a_i, b_i and c_i are the parameters of the membership function, governing the bell-shaped functions, as a result.

In the second layer, the nodes are fixed nodes. They are labeled with M, indicating that they carry out as a simple multiplier. The outputs of this layer can be correspond to as:

$$O_i^2=w_i=\mu_{Ai}(x)\mu_{Bi}(y),i=1,2 \tag{4}$$

which are the called as firing strengths of the rules.

In the third layer, the nodes are also fixed nodes. They are labeled with N, indicating that they play a normalization role to the firing strengths from the preceding layer.

The outputs of this layer can be represented as:

$$O_i^3=\overline{w}_i=\frac{w_i}{w_1+w_2},i=1,2 \tag{5}$$

which are the so-called normalized ring strengths.

In the fourth layer, the nodes are adaptive nodes. The output of each node in this layer is simply the product of the normalized firing strength and a first-order polynomial. Thus, the outputs of this layer are given by:

$$O_i^4=\overline{w}_i f_i=\overline{w}_i(p_i x+q_i y+r_i),i=1,2 \tag{6}$$

In the fifth layer, there is only one single fixed node labeled with S. This node performs the summation of all incoming signals. Hence, the overall output of the model is given by:

$$O_i^5=\sum_{i=1}^{2}\overline{w}_i f_i=\frac{\left(\sum_{i=1}^{2} w_i f_i\right)}{w_1+w_2},i=1,2 \tag{7}$$

It can be experiential that there are two adaptive layers in this ANFIS structural design, that is the first layer and the fourth layer. In the first layer, there are three changeable parameters $\{a_i, b_i, c_i\}$ which are connected to the input membership functions. These parameters are the so-called premise parameters. In the fourth layer, there are also three modifiable parameters $\{p_i, q_i, r_i\}$, pertaining to the first order polynomial. These parameters are so-called consequent parameters (Magesh *et al*., 2011; Katoch, 2004).

TRAINING AND TESTING USING ANFIS CLASSIFIER

Some of the data features are to be taken to identify the normal lung region and COPD affected lung by this the classifier is trained. The data features will then train the classifier and the

classifier will find whether the given CT scan image is normal or abnormal. The data features which have chosen for training the ANFIS classifier are number of cavities in the lung region, maximum area of cavity in the lung region, minimum area of cavity in the lung region, total number of pixels in each cavity, maximum repeated pixel in the cavity regions together and maximum repeated pixel in the lung region. After computing all the data features, have to give the values to the classifier. For instance, choosing three normal CT scan images and three abnormal CT scan images, need to calculate all the six data features separately for all the CT scan images had chosen. After calculating all the six data features for every chosen CT scan images, have to give the result to the ANFIS classifier. Using those results train the classifier to identify the normal and abnormal lung from the given CT scan image. After the ANFIS classifier is trained, give a new CT scan image to find whether it has COPD or not. Afterwards, the six data features such as number of cavities in the lung region, maximum area of the cavity region, minimum area of the cavity region, total number of pixels in each cavity, maximum frequent pixel in the cavity region and maximum repeated pixel in the lung region are calculated for the new CT scan image. The computed values of all the six data features are then give to the ANFIS classifier. The ANFIS classifier is then comparing the values of all the six data features with the stored values of normal and abnormal CT scan images. Because during training have stored all the six data features of the five normal CT scan images and five abnormal CT scan images. After comparison, the ANFIS classifier will identify whether the given CT scan image comes under normal category or abnormal category.

RESULTS AND DISCUSSION

The experimental result is conducted in MATLAB. Figure 9 shows the normal and abnormal lung images.

The sample images are taken and the images are filtered using Adaptive Median filter. The filtering technique is used to remove the noises and it improves the quality of the images as shown in Fig. 10.

The sample images after applied the filtering technique are given to the process of lung segmentation. The lung segmentation process only segments the lung region from the sample CT scan images. Figure 11 shows a sample image of segmented lungs with COPD and without COPD.

After the lung is segmented from the sample images, have to segment the cavities from the lung region. Using the cavities in the lung region identify whether a lung is COPD affected or not.

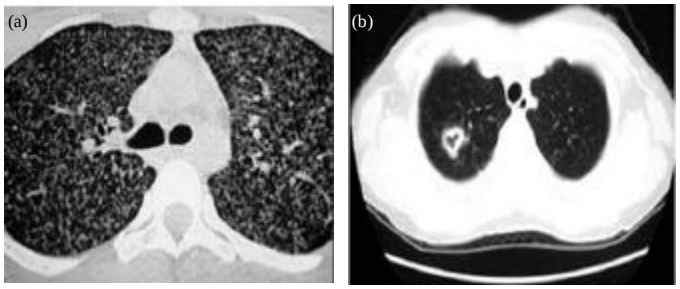

Fig. 9(a-b): Sample images of normal and abnormal lungs images (a) Normal Image and (b) Abnormal image

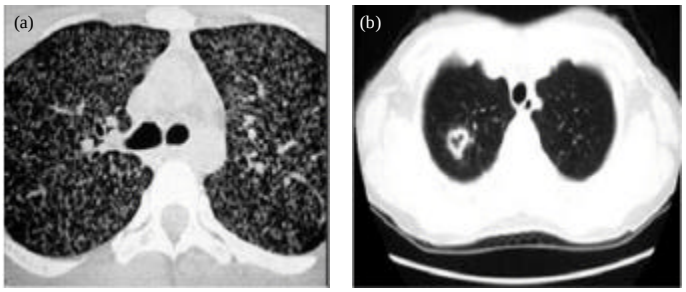

Fig. 10(a-b): Sample image of lungs after filtering process (a) Normal image after filtering process and (b) Abnormal image after filtering process

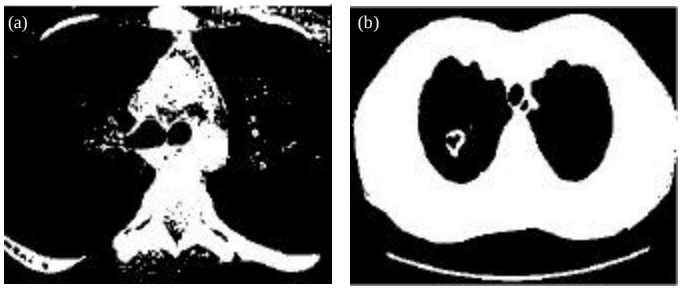

Fig. 11(a-b): Sample image of lungs after segmentation process (a) Normal image after segmentation process and (b) Abnormal image after segmentation process

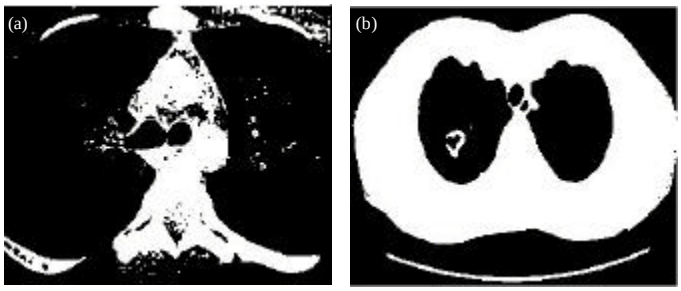

Fig. 12(a-b): Sample image of lungs after segmenting the cavities (a) Normal image after segmenting cavities and (b) Abnormal image after segmenting cavities

Figure 12 shows a sample image of segmented cavities and segmented cavities with CT scan image for the COPD affected lung.

PERFORMANCE ANALYSIS USING EVALUATION METRICS

The evaluation of the COPD identification of the images is carried out using the following metrics:

$$\text{Sensitivity} = TP/(TP+FN)$$

Table 1: Comparative analysis of existing technique with proposed technique

Techniques	TP	TN	FP	FN	Sensitivity	Accuracy
SVM Technique	3	9	1	1	0.9	0.857
Proposed ANFIS	1	4	1	0	0.43	0.989

$$\text{Accuracy} = (TN+TP)/(TN+TP+FN+FP)$$

where, True Positive TP, True Negative TN, False Negative FN, False Positive FP.

Sensitivity is the proportion of true positives that are correctly identified by a diagnostic test. It shows how good the test is at detecting a disease.

Accuracy is the proportion of true results, either true positive or true negative, in a population. It measures the degree of veracity of a diagnostic test on a condition.

Table 1 shows the accuracy comparison between proposed technique and the existing technique. The tabular column shows that the proposed technique gives better performance than the existing technique.

CONCLUSION

In this study, proposed an efficient technique for the detection of COPD in the lungs using CT scan Images. The proposed technique contains pre-processing, lung segmentation, cavity segmentation, feature extraction, training and testing using ANFIS classifier. The ANFIS classifier is efficient and simple in nature. The performance of the proposed technique and the existing technique is analyzed using evaluation metrics. To evaluate these metrics, should need some terms like True Positive, True Negative, False Positive and False Negative. After evaluating these metrics it shows that the performance of proposed technique is better when compared to the existing technique in terms of accuracy. The result shows that the accuracy of proposed technique higher than existing techniques.

REFERENCES

Chen, T. and H.R. Whu, 1998. Space space variant median filters for the restoration of impulse noise corrupted images. IEEE Trans. Image Process., 7: 784-789.

Fukuchi, Y., M. Nishimura, M. Ichinose, M. Adachi and A. Nagai *et al.*, 2004. COPD in Japan: The Nippon COPD epidemiology study. Respirology, 9: 458-465.

Giger, M.L., N. Karssemeijer and S.G. Armato, 2001. Guest editorial computer- aided diagnosis in medical imaging. IEEE Trans. Med. Imaging, 20: 1205-1208.

Gonzales, R.C. and R.E. Woods, 2002. Digital Image Processing. 2nd Edn., Prentice-Hall, New Jersey, USA., ISBN-10: 0201180758.

Jang, J.S.R., 1993. ANFIS: Adaptive-network-based fuzzy inference system. IEEE Trans. Syst. Man Cybern, 23: 665-685.

Katoch, V.M., 2004. Newer diagnostic techniques for tuberculosis. Indian J. Med. Res., 120: 418-428.

Lee, N.A., H. Rusinek, J. Weinreb, R. Chandra, H. Toth, C. Singer and G. Newstead, 1997. Fatty and fibroglandular tissue volumes in the breasts of women 20-83 years old: Comparison of X-ray mammography and computer-assisted MR imaging. Am. J. Roentgenol., 168: 501-506.

Loveymi, S., B. Shadgar and A. Osareh, 2011. An efficient approach to automated medical image annotation. Int. Rev. Comput. Software, 6: 749-759.

Magesh, B., P. Vijayalakshmi and M. Abirami, 2011. Computer aided diagnosis system for the identification and classification of lessions in lungs. Int. J. Comput. Trends Technol., (In Press).

Malik, M.H., S.A.M. Gilani and Anwaar-ul-Haq, 2008. Adaptive Image Fusion Scheme Based on Contourlet Transform and Machine Learning. In: Innovations and Advanced Techniques in Systems, Computing Sciences and Software Engineering, Elleithy, K. (Ed.). Vol. 3, Springer, Netherlands, ISBN: 978-1-4020-8734-9, pp: 313-318.

Maragos, P. and R. Schafer, 1987. Morphological filters-part II: Their relations to median order-statistic and stack filters. IEEE Trans. Acoust., Speech Signal Process., 35: 1170-1184.

Murray, C.J.L. and A.D. Lopez, 1997. Alternative projections of mortality and disability by cause 1999-2020: Golden burden of disease study. Lancet, 349: 1498-1504.

Pauwels, R., A.S. Buist, P. Ma, P.M. Calverley, C.R. Jenkins, S.S. Hurd and GOLD Scientific Committee, 2001. Global strategy for the diagnosis, management and prevention of chronic obstructive pulmonary disease. NHLBI/WHO Global Initiative for Chronic Obstructive Lung Disease (GOLD) Workshop summary. Am. J. Respir. Crit. Care Med., 163: 1256-1276.

Pauwels, R.A. and K.F. Rabe, 2004. Burden and clinical features of chronic obstructive pulmonary disease (COPD). Lancet, 364: 613-620.

Pena, V.S., M. Miravitlles, R. Gabriel, C.A. Jimenez-Ruiz and C. Villasante *et al.*, 2000. Geographic variations in prevalence and underdiagnosis of COPD: results of the IBERPOC multicentre epidemiological study. Chest, 118: 981-989.

Rennard, S., M. Decramer, P.M. Calverley, N.B. Pride, J.B. Soriano, P.A. Vermeire and J. Vestbo, 2002. Impact of COPD in North America and Europe in 2000: Subjects' perspective of confronting COPD international survey. Eur. Respir. J., 20: 799-805.

Sluimer, I.C., P.F. van Waes, M.A. Viergever and B. van Ginneken, 2003. Computer-aided diagnosis in high resolution CT of the lungs. Med. Phys., 30: 3081-3090.

Stang, P., E. Lydick, C. Silberman, A. Kempel and E.T. Keating, 2000. The prevalence of COPD: using smoking rates to estimate disease frequency in the general population. Chest, 117: 354S-359S.

Uchiyama, Y., S. Katsuragawa, H. Abe, J. Shiraishi and F. Li *et al.*, 2003. Quantitive computerised analysis of diffuse lung disease in high-resolution computed tomography. Med. Phys., 30: 2440-2453.

Viegi, G., A. Scognamiglio, S. Baldacci, F. Pistelli and L. Carrozzi, 2001. Epidemiology of chronic obstructive pulmonary disease (COPD). Respiration, 68: 4-19.

Xie, S., S. Shan, X. Chen and J. Chen, 2010. Fusing local patterns of Gabor magnitude and phase for face recognition. IEEE Trans. Image Process., 19: 1349-1361.